

Document downloaded from:

<http://hdl.handle.net/10251/141426>

This paper must be cited as:

Almeida De-Godoy, V.; Zuquette, L.; Gómez-Hernández, JJ. (2019). Stochastic upscaling of hydrodynamic dispersion and retardation factor in a physically and chemically heterogeneous tropical soil. *Stochastic Environmental Research and Risk Assessment*. 33(1):201-216. <https://doi.org/10.1007/s00477-018-1624-z>



The final publication is available at

<https://doi.org/10.1007/s00477-018-1624-z>

Copyright Springer-Verlag

Additional Information

1 **Stochastic Upscaling of Hydrodynamic Dispersion and Retardation Factor in a**
2 **Physically and Chemically Heterogeneous Tropical Soil**

3 Vanessa A. Godoy^{1,2*}, Lázaro Valentin Zuquette¹ and J. Jaime Gómez-Hernández²

4 ¹ Geotechnical Engineering Department, São Carlos School of Engineering, University of
5 São Paulo. Avenida Trabalhador São Carlense, 400, 16564-002, São Carlos, São Paulo,
6 Brazil.

7 ² Institute for Water and Environmental Engineering, Universitat Politècnica de València,
8 Camí de Vera, s/n, 46022, València, Spain

9 * corresponding author: valmeida@usp.br (+55)16 35739501

10 **Abstract**

11 Stochastic upscaling of flow and reactive solute transport in a tropical soil is performed
12 using real data collected in the laboratory. Upscaling of hydraulic conductivity, longitudinal
13 hydrodynamic dispersion, and retardation factor were done using three different
14 approaches of varying complexity. How uncertainty propagates after upscaling was also
15 studied. The results show that upscaling must be taken into account if a good reproduction
16 of the flow and transport behavior of a given soil is to be attained when modeled at larger
17 than laboratory scales. The results also show that arrival time uncertainty was well
18 reproduced after solute transport upscaling. This work represents a first demonstration of
19 flow and reactive transport upscaling in a soil based on laboratory data. It also shows how
20 simple upscaling methods can be incorporated into daily modeling practice using
21 commercial flow and transport codes.

22 **Keywords: column experiments, spatial variability, macrodispersion coefficient,**
23 **hydraulic conductivity upscaling, stochastic analysis**

24

25 **1. Introduction**

26 Solute transport numerical modeling is a powerful tool to predict aquifer response in a
27 remediation plan, to evaluate the impact of a radioactive underground repository on the
28 biosphere, to verify the efficacy of geological materials to be used as liners in landfills, to

1 assess health risks due contaminant exposure, or to be used in decision-making
2 processes (Bellin et al., 2004; Dagan, 2004; Feyen et al., 2003a, 2003b). Numerical
3 models require input parameters that must be determined reliably to guarantee the quality
4 of their predictions (Willmann et al., 2006).

5 Hydraulic conductivity (K) and transport parameters such as hydrodynamic dispersion
6 coefficient (D), dispersivity (α) and retardation factor (R) are, generally, determined in the
7 laboratory at a scale of a few centimeters (fine scale) (Jarvis, 2007; Jellali et al., 2010;
8 Logsdon Keller and Moorman, 2002; Osinubi and Nwaiwu, 2005; Tuli et al., 2005;
9 Vanderborght et al., 2000). Modeling water flow and solute transport at a fine-scale
10 resolution is impractical, especially when modeling must be repeated many times, such
11 as in stochastic analyses (Feyen et al., 2003a; Lawrence and Rubin, 2007).

12 Numerical simulations are performed in a scale of meters to kilometers (coarse scale),
13 using equivalent parameters, homogeneous in each model cell (Wen and Gómez-
14 Hernández, 1996). This implies a simplification of the problem since not all fine-scale
15 information is transferred to the coarse scale (Bellin et al., 2004; Fernández-Garcia and
16 Gómez-Hernández, 2007). In addition, the lack of exhaustive information implies
17 uncertainty on flow and transport predictions, which should also be taken into account
18 when performing upscaling (Fernández-Garcia and Gómez-Hernández, 2007; Gómez-
19 Hernández and Wen, 1994; Li et al., 2011a).

20 We face two main problems in solute transport modeling. The first one is how to treat
21 parameter spatial heterogeneity and the second one is how to account for the difference
22 of scales between measurements and modeling scales (Dagan, 1989; Gómez-
23 Hernández et al., 2006; Taskinen et al., 2008). The first problem can be tackled by using
24 geostatistical techniques such as simulation or estimation that permit a coherent
25 assignment of values at locations where measurements were not taken based on the
26 values observed at measurement locations (Capilla et al., 1999; Cassiraga et al., 2005;
27 Journel and Gomez-Hernandez, 1993; Li et al., 2011b; Morakinyo and Mackay, 2006;
28 Wen et al., 1999; Zhou et al., 2012, 2010). The second problem can be solved by defining
29 upscaling rules that incorporate subgrid heterogeneity of the parameters that control flow
30 and solute transport, and that transfer the information obtained at the fine scale onto the

1 coarse scale to be used in the numerical code (Deng et al., 2013; Fernàndez-Garcia and
2 Gómez-Hernández, 2007; Li et al., 2011b).

3 The upscaling of hydraulic conductivity is well established in the literature and several
4 approaches have been reported, showing the limitations and effectiveness of local and
5 non-local upscaling methods for the reproduction of water flow patterns under different
6 types of heterogeneity (Cadini et al., 2013; Cassiraga et al., 2005; Fernàndez-Garcia and
7 Gómez-Hernández, 2007; Gómez-Hernández et al., 2006; Li et al., 2011a; Lourens and
8 van Geer, 2016; Renard and de Marsily, 1997; Sánchez-Vila et al., 1996; Selvadurai and
9 Selvadurai, 2014; Wen and Gómez-Hernández, 1996). However, upscaling hydraulic
10 conductivity only is not enough to reproduce the fine-scale transport behavior at the
11 coarse scale due to the loss of K heterogeneity present at the fine scale that influences
12 solute transport behavior (Cassiraga et al., 2005; Journel et al., 1986; Scheibe and
13 Yabusaki, 1998). Fernàndez-Garcia and Gómez-Hernández (2007) proposed a method
14 to compensate for the loss of information due to hydraulic conductivity upscaling,
15 consisting of introducing an enhanced block hydrodynamic dispersion tensor and found
16 that the median travel times of the breakthrough curves (BTC) were well reproduced but
17 the tails were not.

18 While less common than flow upscaling studies, some solute transport upscaling works
19 can be found in the literature showing the characteristics and limitations of different
20 transport upscaling methods using deterministic and stochastic approaches of varying
21 complexity (Bellin et al., 2004; Cadini et al., 2013; Cassiraga et al., 2005; Fernàndez-
22 Garcia et al., 2009; Fernàndez-Garcia and Gómez-Hernández, 2007; Gómez-Hernández
23 et al., 2006; Moslehi et al., 2016; Salamon et al., 2007; Tyukhova and Willmann, 2016;
24 Vishal and Leung, 2017; Xu and Meakin, 2013).

25 Most transport upscaling studies are based on synthetic experiments for nonreactive
26 solute transport and focus on the upscaling of only a single transport parameter, for
27 example, the hydrodynamic dispersion or the retardation factor. There is still a lack of
28 studies that intend to define upscaling rules based on real data from laboratory
29 experiments of reactive solute transport in heterogeneous soils. In addition, to the best of
30 our knowledge, performing upscaling considering at the same time the heterogeneity of

1 dispersivity and retardation factor at the local scale has not been discussed in the
2 literature. Determining equivalent transport parameters in tropical soils, present in many
3 regions of the world and related to important engineering problems, has not been
4 performed before; this is a gap we also aim to reduce.

5 The purpose of this study is to propose upscaling rules for reactive solute transport, using
6 fine-scale data obtained at the laboratory from water flow and reactive solute transport
7 experiments using undisturbed tropical soil columns. We must clarify that in this work we
8 are not investigating chemical reactions but only sorption (due to physical retention and/or
9 adsorption) (Freeze and Cherry, 1979). A solute will be considered nonreactive when the
10 retardation factor, R , is equal to one, while it will be considered reactive when is larger
11 than one.

12 Differently from earlier studies (Fernández-García et al., 2009; Fernández-García and
13 Gómez-Hernández, 2007), we use a Simple Laplacian-with-skin method to upscale
14 hydraulic conductivity (Gómez-Hernández, 1990; Li et al., 2011b) in order to obtain the
15 best reproduction of water flow as observed at the fine scale. In line with the work by
16 Fernández-García and Gómez-Hernández (2007), we use the Enhanced
17 Macrodispersion Coefficient approach but, as a novelty, the determination of the
18 macrodispersion coefficient was made by considering also the heterogeneity of
19 dispersivity, α , at the local scale. To study the upscaling of retardation factor, the p -norm
20 approach, i.e., power averaging of the cell values within the block, was used to compute
21 an equivalent R after a prior analysis to determine an optimal exponent p (Gómez-
22 Hernández et al., 2006a). Contrasting with the majority of previous studies that focused
23 on a single realization, we perform a stochastic analysis to study the variability of the
24 upscaled parameters but also the propagation of uncertainty after upscaling. The
25 assessment of the upscaled models is based on the reproduction at the coarse scale of
26 the breakthrough curves (BTC) obtained at the fine scale at a selected control plane.

27 **2. Upscaled transport model**

28 The Macrodispersion method as described by Fernández-García and Gómez-Hernández
29 (2007) was used to upscale the local-scale hydrodynamic dispersion, thus accounting for

1 the reduction of within-block heterogeneity. The retardation factor was upscaled using the
 2 p-norm approach. These two methods were used for their simplicity and for its readiness
 3 to use in commercial transport codes based on the classical advection-dispersion
 4 equation (ADE). In this section, some details about them are provided. We recognize that
 5 sometimes the use of the ADE at the coarse scale may be inadequate to reproduce
 6 reactive solute transport at the fine scale, as discussed in previous studies (Fernàndez-
 7 Garcia et al., 2009; Li et al., 2011b). Because of that, we also intend to show the possible
 8 limitations of the use of the ADE to upscale transport solute parameters.

9 **2.1. Hydrodynamic dispersion upscaling using the ADE**

10 At the fine scale, the flow equation, assuming steady-state flow in the absence of sinks
 11 and sources for an incompressible fluid in a saturated porous media, is given by

$$\nabla \cdot (\mathbf{K}^f(\mathbf{x}) \nabla h(\mathbf{x})) = 0. \quad (1)$$

12 This equation results of combining Darcy's Law and the continuity equation, where h is
 13 the piezometric head, \mathbf{K}^f is a second-order symmetric hydraulic conductivity tensor
 14 (observed at the fine scale), \mathbf{x} represents the spatial location, ∇ is the gradient operator,
 15 and $\nabla \cdot$ the divergence operator.

16 Assuming that Fick's law is appropriate at the local scale, solute transport is given by the
 17 ADE equation, which is a mass balance equation, written, for a nonreactive solute, as

$$n^f \frac{\partial C(\mathbf{x}, t)}{\partial t} = -\nabla \cdot (\mathbf{q}(\mathbf{x}) C(\mathbf{x}, t)) + \nabla \cdot (n^f \mathbf{D}^f \nabla C(\mathbf{x}, t)), \quad (2)$$

18 where \mathbf{q} is the Darcy velocity given by $\mathbf{q}(\mathbf{x}) = -\mathbf{K}^f(\mathbf{x}) \nabla h(\mathbf{x})$, n^f is the porosity, C is the
 19 solute concentration, and \mathbf{D}^f is the local hydrodynamic dispersion coefficient tensor with
 20 eigenvalues given by

$$\mathbf{D}_i^f = D_m + \alpha_i \frac{|\mathbf{q}^f|}{n^f}, \quad (3)$$

21 where D_m is the effective molecular diffusion coefficient and α_i are the local dispersivity
 22 coefficients. The dispersivity values parallel and transverse to the flow direction are
 23 designated as longitudinal and transverse dispersivities, α_L and α_T .

1 Eq.(1)(1) and Eq.(2) are used to solve the water flow and transport equations at the fine
 2 scale, respectively. However, due to the need to solve those problems on a grid coarser
 3 than the scale of the measurements, it is necessary to use block equivalent parameters
 4 (hereafter, block properties will be identified by the subscript b). According to Fernàndez-
 5 Garcia and Gómez-Hernández (2007), a block equivalent hydraulic conductivity tensor,
 6 \mathbf{K}_b , must preserve the fine-scale average flux through the block. Whereas a block
 7 equivalent hydrodynamic dispersion tensor, \mathbf{D}_b , should consider not only the dispersive
 8 fluxes at the fine scale (herein referred to as fine scale hydrodynamic dispersion) but also
 9 should account for the loss of spreading caused by the homogenization of the hydraulic
 10 conductivities. The enhanced block hydrodynamic dispersion tensor \mathbf{D}_b includes an
 11 equivalent fine-scale local dispersivity (α_{eq}) plus a macrodispersivity term (A_i), which is
 12 computed so as to increase the dispersion in the upscaled (homogeneous) block. Using
 13 α_{eq} and A_i to compute \mathbf{D}_b is known as the Macrodispersion approach; the resulting
 14 macrodispersion tensor is

$$\mathbf{D}_b = \mathbf{D}_m + (\alpha_{eq} + A_i) \frac{|\mathbf{q}^f|}{n^f} \quad (4)$$

15 The term A_i is constant over time but varies in space among blocks. According to Gelhar
 16 et al. (1992), A_i can range from meters to kilometers while α_{eq} ranges in the order of
 17 millimeters. Based on a literature review, Zech et al. (2015) showed that
 18 macrodispersivities can range from millimeters to meters. In this paper, block equivalent
 19 dispersivities will be named $\alpha_b = \alpha_{eq} + A_i$.

20 In the macrodispersion approach, upscaling is based on the macrodispersion concept
 21 (Gelhar and Axness, 1983) and the resulting transport equation to be used at the coarse
 22 scale has the same form as the local ADE at the fine scale, but replacing the local
 23 hydrodynamic dispersion tensor by the new macrodispersion tensor.

24 **2.2. Upscaling of the retardation factor**

25 The governing equation of solute transport subject to advection, hydrodynamic
 26 dispersion, and sorption in a physically and chemically heterogeneous aquifer at the fine
 27 scale can be expressed as

$$\frac{\partial C(\mathbf{x},t)}{\partial t} + \frac{\rho_d}{n^f} \frac{\partial S(\mathbf{x},t)}{\partial t} = -\frac{1}{n^f} \nabla \cdot (\mathbf{q}(\mathbf{x})C(\mathbf{x},t)) + \frac{1}{n^f} \nabla \cdot (\mathbf{D}^f \nabla C(\mathbf{x},t)), \quad (5)$$

1 where ρ_d is the matrix bulk density and S is the nonaqueous-phase concentration of
 2 sorbed solutes. The relation between C and S is established through a sorption isotherm.
 3 The simplest sorption isotherm function assumes that sorption is instantaneous,
 4 reversible and that the concentration of sorbed solutes onto the solid is directly
 5 proportional to the concentration of dissolved solutes (Freeze and Cherry, 1979). The
 6 constant of proportionality between C and S is the distribution coefficient (K_d)

$$K_d(x) = \frac{S(x)}{C(x)} \geq 0, \quad (6)$$

7 which quantifies the interaction between the contaminants and the soil particles. This
 8 parameter is spatially variable and its variation can exert a key role in the behavior of the
 9 solute plumes (Brusseu, 1998; Brusseu and Srivastava, 1999; Robin et al., 1991).
 10 There is no consensus about the cross-correlation between K_d and K . According to Robin
 11 et al. (1991), this correlation, in real fields, may range from weakly negative to mildly
 12 positive. In the studied soil, a very weakly negative correlation between $\ln K$ and K_d was
 13 found (-0.02) and because of that, we assumed no correlation between them.

14 The retardation factor R is related to K_d by,

$$R(x) = 1 + \frac{\rho_d}{n^f(x)} K_d(x), \quad (7)$$

15 and can be interpreted as the ratio of the average fluid velocity (v) ($v = q(x)/n^f$) to the
 16 velocity at which the solute propagates (v_s) (Freeze and Cherry, 1979)

$$R(x) = \frac{v}{v_s} \geq 1. \quad (8)$$

17 When the solutes do not interact with the solid medium (i.e., they are nonreactive), $R = 1$.
 18 Solutes with $R > 1$ are called reactive solutes (Freeze and Cherry, 1979; Shackelford,
 19 1994).

20 It is important to mention that in FEFLOW (the computer code used in this work) R is
 21 expressed as a function of the Henry's adsorption constant, k [-], as

$$R(x) = 1 + \frac{1-n^f}{n^f} k(x). \quad (9)$$

1 Including R in the transport equation by combining Eq. (5) and Eq. (7) results in the
 2 reactive transport equation given by:

$$\frac{\partial C(\mathbf{x},t)}{\partial t} R(x)n^f + \nabla \cdot (n^f v(x)C(\mathbf{x},t)) = \nabla \cdot (\mathbf{D}^f \nabla C(\mathbf{x},t)). \quad (10)$$

3 The information obtained at the fine scale cannot be used directly at the coarse scale and
 4 it is necessary to calculate a block equivalent retardation factor R_b representative of the
 5 heterogeneity of the retardation factor within the block. This block value must be able to
 6 reproduce the mass flux breakthrough curve (BTC) obtained at the fine scale simulation
 7 when applied to the transport equation with homogeneous parameters within model
 8 blocks at the coarse scale.

9 Since the reproduction of the complete BTC is impossible to achieve, it is necessary to
 10 select which part of the BTC one would like to reproduce best, according to the objective
 11 of the numerical modeling (Gómez-Hernández et al., 2006).

12 For the calculation of R_b , the p-norm (power averaging) of $R(x)$ can be used

$$R_b = \left(\frac{1}{V} \int_V R_f^p(\mathbf{x}) d\mathbf{x} \right)^{\frac{1}{p}}, \quad (11)$$

13 where V indicates the volume of the block and R_f represents the retardation factors at the
 14 fine scale. Depending on the power exponent used, the p-norm will be more affected by
 15 the low values, or by the high values within the block. In this approach, the challenge is
 16 to find the exponent p that will result in an R_b that best reproduces, at the coarse scale,
 17 the transport observed at the fine scale; to find it, numerical simulations must be
 18 performed. This technique follows the line of the power averaging equation used for
 19 calculating equivalent hydraulic conductivity by (Gómez-Hernández and Gorelick, 1989;
 20 Journal et al., 1986).

1 **3. Field characterization**

2 **3.1. Studied soil**

3 The studied tropical soil is found on lithologies belonging to the Botucatu Formation in
4 São Carlos City (21°51'38" S, 47°54'14" W), located in the East-Center of São Paulo State
5 (Brazil). It consists of fine-grained to medium-sized sandstones, with a reddish color, well-
6 selected grains, high sphericity, and very friable or silicified. Cenozoic sediments are the
7 parental material of the studied soil and cover the Botucatu Formation. These sediments
8 are constituted by unconsolidated sands with a thickness ranging from 5 m to 7 m, and
9 can be found in the interior of São Paulo (Azevedo et al., 1981; Giacheti et al., 1993).

10 The study area is a parallelepiped with dimensions $\Delta x = 12$ m, $\Delta y = 8$ m, and $\Delta z = 4$ m,
11 from where the soil samples were taken. At the laboratory, the soil was characterized as
12 clayey sand with macropores and double porosity fabric, an important characteristic in
13 terms of water flow and solute transport. The main minerals present in the studied soil
14 are quartz, kaolinite, and gibbsite, what is in accordance with Giachetti *et al.* (1993) and
15 Kronberg *et al.* (1979). We found a small average amount of organic matter (2.40%) in
16 this soil, common in lateritic acidic soils (Mahapatra et al., 1985). Average values of 5.71
17 and 5.19 for pH in H₂O and KCl, were obtained, respectively, therefore, the soil can be
18 considered strongly acidic, a typical characteristic of Cenozoic sediments and lateritic
19 soils (Fagundes and Zuquette, 2011; Giacheti et al., 1993).

20 The negative ΔpH (-0.52) and a point of zero charge (PZC) (4.67) lower than the $\text{pH}_{\text{H}_2\text{O}}$
21 indicate a predominance of negative charges, which can promote cation adsorption
22 (Fagundes and Zuquette, 2011). The soil has a low cation exchange capacity (CEC)
23 (mean value of 2.51 cmolc Kg⁻¹ and maximum value of 4.20 cmolc Kg⁻¹), suggesting a
24 low capacity to adsorb cations by electrostatic adsorption (Fagundes and Zuquette,
25 2011).

26 **3.2. Experimental determination of water flow and transport parameters**

27 In order to characterize the hydraulic conductivity and the transport parameters, 55
28 undisturbed cylindrical soil samples of 0.10 m diameter and 0.15 m height were taken in

1 the domain described earlier. In the laboratory, K was measured under constant-head
2 conditions, with a hydraulic gradient equal to one, using a rigid-wall permeameter, at a
3 constant temperature of 20 °C.

4 The total porosity was computed as $n_t = 1 - \rho_d / \rho_s$, where ρ_s is the particle density, calculated
5 as 2.71 Mg·m⁻³. The effective porosity, used in the transport model, is equal to the total
6 porosity minus the porosity that corresponds to the soil water content at 33 kPa, a suction
7 equivalent to the field capacity (Ahuja et al., 1984; Brutsaert, 1967; Corey, 1977;
8 Dippenaar, 2014).

9 When steady-state flow was reached in the flow tests, miscible displacement tests were
10 performed. A solution 2.56 mol m⁻³ KCl (made up of 100 mg L⁻¹ K⁺ and 90.7 mg L⁻¹ Cl⁻,
11 and referred to as the initial concentration, C₀) was continuously injected into the soil
12 column. Solute displacement tests were also carried out under constant hydraulic head
13 and isothermal (20 °C) conditions. The concentration (C) was measured at preset time
14 intervals and the BTC's were determined at the outlet. Since in this work we are interested
15 in reactive transport, only the results related to the reactive solute (potassium ion, K⁺) are
16 discussed.

17 The advection-dispersion equation (ADE) used to interpret the BTCs is

$$R \frac{\partial C}{\partial t} = D \frac{\partial^2 C}{\partial x^2} - v \frac{\partial C}{\partial x}, \quad (12)$$

18 where C is the solute concentration [ML⁻³], D is the hydrodynamic dispersion coefficient
19 [M²T⁻¹], R is the retardation factor [-], x is the distance [L], and t is the time [T].

20 When the initial condition is C = 0 for the entire sample, and the boundary conditions are
21 C = C₀ at the inlet and C = 0 at an infinite distance from the inlet, Eq (12) has the following
22 analytical solution,

$$\frac{C(t)}{C_0} = \frac{1}{2} \left[\operatorname{erfc} \left(\frac{RL - vt}{2\sqrt{DRt}} \right) \right] + \frac{1}{2} \exp \left(\frac{vL}{D} \right) \operatorname{erfc} \left(\frac{RL + vt}{2\sqrt{DRt}} \right), \quad (13)$$

23 where $\operatorname{erfc}(\cdot)$ is the complementary error function

24 This expression was fitted to the observed BTCs for each soil sample and values of the
25 hydrodynamic dispersion and the retardation factor were obtained for both K⁺ and Cl⁻.
26 The fitting was performed using the computer program CFITM (van Genuchten, 1980),

1 that is part of the Windows-based computer software package Studio of Analytical Models
2 (STANMOD) (Šimůnek et al., 1999). From the values of the hydrodynamic dispersion
3 obtained after the fitting, the dispersivity values were calculated using the relation

$$D = \alpha \cdot v. \quad (14)$$

4 The fit of the experimental BTC to the ADE model was evaluated by its R^2 . Most BTCs
5 presented significant tailing, R^2 ranged from 0.77 to 0.99 with a mean of 0.92. We
6 conclude that the experimental data can be properly described by the ADE model.

7 **3.3. Spatial variability**

8 The exploratory statistics of the 55 measurements of the studied variables (K , n , α , and
9 R) are summarized in Table 1. K , R and α displayed high variability (Fu and Gómez-
10 Hernández, 2009; Robin et al., 1991; Wilding and Drees, 1983), on the contrary, the
11 porosity presented a very low variability (Wilding and Drees, 1983).

12 The measured K and α values are best fitted by lognormal distributions. The lognormal
13 model implies that the natural logarithms of K ($\ln K$) and α ($\ln \alpha$) are modeled by Gaussian
14 distributions. The normality of $\ln K$ and $\ln \alpha$ was confirmed by the Kolmogorov-Smirnov test
15 with a 95% confidence interval. The measured porosity and retardation factor could not
16 be fitted by a normal distribution and they were transformed into normal variables using
17 an empirical anamorphosis (also known as a normal-score transform). All transformed
18 variables were standardized to normal distributions of mean zero and variance one.
19 Variogram analysis was performed in the standardized variables $\ln K$, n , $\ln \alpha$, and R .

20 Geostatistical techniques were used to build a model of the spatial variability of the
21 parameters with the purpose of estimating the properties at unsampled locations
22 (Goovaerts, 1999). The theory of geostatistics is based on the random function model
23 assumption, where variables are modeled as spatially correlated random variables.
24 Within this framework, it is possible to perform coherent inferences about a variable and
25 its spatial variability.

26 Using the Stanford Geostatistical Modeling Software (SGeMS) (Remy, 2004), we
27 conclude that the 55 measurements showed a spatial variability that can be modeled by
28 an isotropic spherical variogram of the form

$$\gamma(\mathbf{h})=c_0+c_1.\text{sph}(|\mathbf{h}|,a), \quad (15)$$

1 where a is the range, c_0 is the nugget effect, c_1 is the sill, \mathbf{h} is the directional lag distance,
2 and $\text{sph}(\cdot)$ is the spherical function. We have decided to use an isotropic variogram after
3 investigating the ranges of the variograms in several directions and observing that there
4 is no a significant difference on the continuity patterns as orientation changes. Due to the
5 limited number of samples in the vertical direction, we assumed that the spatial correlation
6 obtained for the horizontal direction is the same in the vertical direction. This choice can
7 also be justified by the absence of clear anisotropies in the soil; it is well known that the
8 spatial correlation anisotropy is, among other reasons, the responsible for the flow
9 anisotropy (Lake, 1988). Table 2 shows the parameters of the variogram models used to
10 fit the isotropic experimental variograms.

11 The variograms of the solute transport parameters contain a nugget effect, which implies
12 short-scale spatial variability and/or measurement error. According to the nugget-to-total-
13 sill ratio classification, these variables had a moderate spatial dependence (Cambardella
14 et al., 1994).

15 **4. Numerical simulations**

16 **4.1. Simulation of the random fields**

17 Within the random field theory (Griffiths and Fenton, 2008; Vanmarcke, 1983), the
18 variables, $\ln K$, $\ln \alpha$, n —actually its normal-score transform—, and R —actually, its normal-
19 score transform—are modeled as random variables at each location in space. These
20 random variables are represented by a probability density function (pdf) that measures
21 the likelihood that the random variable takes a specific value at a given location
22 (Cassiraga et al., 2005). First- and second-order stationary Gaussian random fields were
23 used to model all variables. A Gaussian random field is completely defined by its first two
24 moments, mean and variance, and its autocorrelation function, and it is represented by
25 the infinite set of multivariate Gaussian distributions that can be built with any combination
26 of points within some spatial domain (Griffiths and Fenton, 2008; Vanmarcke, 1983).

27 Thirty equally-likely and conditioned realizations of $\ln K$, n , $\ln \alpha$ and R were generated using
28 the Sequential Gaussian Simulation (SGS) algorithm as implemented in the code

1 GCOSIM3D (Gómez-Hernández and Journel, 1993) using the variogram functions whose
2 parameters are shown in Table 2. The lnK random field domain is a parallelepiped with
3 dimensions of $\Delta x = 24$ m, $\Delta y = 16$ m and $\Delta z = 8$ m and it is discretized in 3 072 000 cubic
4 cells of side 0.1 m; each cell is of the magnitude of the permeameter measurements. The
5 lnK domain is twice the size of the studied area because the lnK upscaling technique
6 demands a skin composed by a certain number of additional elements (Gómez-
7 Hernandez, 1990). However, only the inner domain of size $\Delta x = 12$ m, $\Delta y = 8$ m and $\Delta z =$
8 4 m was used to simulate and compare flow at the coarse and fine scales. The random
9 fields of the other variables, conditioned on the 55 measurements, were generated in a
10 domain equal to the studied area ($\Delta x = 12$ m, $\Delta y = 8$ m and $\Delta z = 4$ m) and discretized in
11 384 000 cubic cell of side 0.1 m since no skin was necessary in their upscaling methods.

12 The number of realizations analyzed here may be considered small for performing a
13 rigorous estimation of uncertainty. However, since our objective is to identify trends and
14 the impact of the upscaling in uncertainty propagation, we believe that a set of 30
15 realizations is enough. Before performing water flow and solute transport numerical
16 simulations, all realizations were back-transformed according to the cumulative
17 distribution functions of the measured data. Fig. 1a-d shows the realization number 1 of
18 all variables (in real space, that is, after back transformation) K, n, α and k (Henry
19 coefficient related to R by Eq. (9)).

20 **4.2. Flow and transport solutions**

21 The finite element method (FEM) with a pre-conditioned conjugate-gradient algorithm as
22 implemented in FEFLOW 7.1 was used to solve the water flow and solute transport for
23 each one of the 30 realizations (Diersch, 2014). The realizations of hydraulic conductivity
24 were used as input parameter to the flow model while the realizations of dispersivity and
25 retardation factor were used as input parameters to the solute transport models. We
26 recognize that the effect of a heterogeneous variable porosity can affect the solute
27 transport behavior, but, due to its very low variability (see Table 2) and to the necessity
28 to reduce the dimensionality of the problem, a homogeneous value of porosity, equal to
29 the arithmetic mean of the 55 observations, was considered for all numerical models at
30 the fine scale.

1 The numerical domain is a parallelepiped discretized into 120 x 80 x 40 cubic cells of 0.1
2 m by 0.1 m by 0.1 m for a total of 384 000 elements. The transport mapping method (also
3 called transfinite interpolation) algorithm was used to generate the rectangular mesh.

4 Steady-state flow was simulated by considering a confined problem under a constant
5 gradient set to one to reproduce the laboratory conditions. The boundary conditions were
6 no-flow at the top and bottom faces and constant-head was set equal to 50 m at the left
7 face and to 38 m at the right face, forcing flow from left to right. The specific discharge in
8 the x-direction (q_x) was calculated for each realization at a control plane, positioned on
9 the exit face, orthogonal to the flow direction.

10 Reactive solute transport was simulated by adopting a first-type boundary condition at the
11 left side, using a mass concentration of 100 mg/L (Fig. 2). At the top and bottom faces,
12 no mass flow boundary condition was assumed. The solute transport was modeled as
13 transient for a period of 35 days for the nonreactive problems and 100 days for the
14 reactive ones. The time discretization was made based on a grid Courant number of 0.04.
15 The BTCs were obtained at the exit plane of the domain (right side).

16 **4.3. Upscaling of water flow**

17 A Simple Laplacian-with-skin method was used to upscale the hydraulic conductivity
18 (Gómez-Hernandez, 1990; Li et al., 2011b) in order to obtain the best reproduction of
19 water flow at the fine scale. The whole domain, heterogeneous at the fine scale, was
20 replaced by a unique homogeneous block, i.e., the size of the equivalent block coincides
21 with the field site extension without intermediate resolutions (both for water flow and
22 solute transport). The effectiveness of K upscaling was evaluated by comparing the mean
23 specific discharge in the x-direction (q_x) at the control plane computed at the fine and
24 coarse scales, and it was quantified by the relative bias of the specific discharge (RB_q)

$$RB_q = \frac{1}{NR} \sum_{i=1}^{NR} \left| \frac{q_{f,i} - q_{c,i}}{q_{f,i}} \right| 100, \quad (16)$$

25 where NR is the number of realizations; $q_{f,i}$ is the specific discharge through a control
26 plane obtained from the numerical modeling at the fine-scale for realization i, and $q_{c,i}$ is
27 the specific discharge through the same control plane at the coarse-scale for realization i.

1 4.4. Upscaling of hydrodynamic dispersion

2 The upscaling of hydrodynamic dispersion was done by using the Macrodispersion
3 approach. According to this, to determine the block equivalent hydrodynamic dispersion
4 (D_b) it is necessary to calculate α_b , that is, the sum of the equivalent fine-scale local
5 dispersivity (α_{eq}) plus the macrodispersivity term (A_i). Both A_i and α_{eq} were calculated
6 based on the first- and second-order moments of the BTC at the exit plane (positioned on
7 the far right of the domain), using the expression (Wen and Gómez-Hernández, 1998)

$$\alpha_{eq} \text{ or } A_i = \frac{L \sigma_t^2}{2 T_a^2}, \quad (17)$$

8 where L is the block length, T_a is the average of the arrival times, and σ_t^2 is the variance
9 of the arrival times.

10 The determination of the α_{eq} and A_i was made by solving a local transport problem
11 releasing solute mass from one side of the block and collecting it at the opposite side,
12 then, T_a and σ_t^2 were computed from the BTC at the exit plane. We used two scenarios
13 of nonreactive solute transport to obtain α_b . In scenario 1, first, for each realization at the
14 fine scale, purely advective transport was solved by using a heterogeneous K , allowing
15 us to calculate the macrodispersion coefficients associated with the heterogeneity of K
16 (A_i). Second, K was assumed homogeneous, and transport was solved with a
17 heterogeneous α , allowing us to calculate the equivalent dispersivities (α_{eq}). Lastly, A_i and
18 α_{eq} were summed up to give the α_b . In short, in scenario 1, we determined separately α_{eq}
19 and A_i and then added them up to calculate α_b . In scenario 2, the heterogeneity at the
20 local scale of both K and α was simultaneously considered and, for each realization, a
21 transport problem at the local scale was solved from which α_b was directly determined
22 using Eq. (17). Table 3 summarizes the conditions adopted in each scenario. Fig. 3 shows
23 a cross-plot between the α_b determined in both scenarios. The results show that
24 approach in scenario 2 can be used to quantify directly the effects of the local-scale
25 heterogeneity of both α and K , since the results obtained by the two scenarios are very
26 similar, with a relative bias of only 4.2 %.

1 The performance of hydrodynamic dispersion upscaling was evaluated by comparing the
 2 BTCs at the exit plane obtained from the fine- and coarse-scale models. These
 3 comparisons were also done for a few points of the BTC, more precisely, at the mean
 4 (T_{mean}), 5% (early, $T_{05\%}$), 50% (median $T_{50\%}$) and 95% (late, $T_{95\%}$) arrival times. It is
 5 important to mention that the selection of the part of BTC used to calculate the upscaled
 6 transport parameters is a very important step for the correct application of upscaled
 7 transport parameters in daily practice. According to Fu and Gómez-Hernández (2009)
 8 and Gómez-Hernández et al. (2006), early arrival times must be well reproduced if, for
 9 example, the objective of the transport model is the design of an underground repository
 10 for toxic or radioactive waste; median arrival times, if the objective is to assess health risks
 11 associated with contaminant exposure by drinking water (Lemke et al., 2004), and late
 12 arrival times, if the objective is to design a remediation plan. Failing to take this into
 13 account will yield under- or overestimation of the arrival times critical for the purposes of
 14 the study.

15 For each arrival time mentioned before, the mismatch between the concentrations
 16 obtained at the fine and coarse scales was quantified by the relative bias of the
 17 hydrodynamic dispersion (RB_d), expressed as

$$RB_d = \frac{1}{NR} \sum_{i=1}^{NR} \left| \frac{C_{f,i} - C_{c,i}}{C_{f,i}} \right| 100, \quad (18)$$

18 where $C_{f,i}$ is the concentration through a control plane obtained from the numerical
 19 modeling of a nonreactive solute at the fine scale for realization i , and $C_{c,i}$ is the
 20 concentration of the same nonreactive solute through the same control plane at the
 21 coarse-scale for the same realization.

22 The uncertainty analysis of the nonreactive solute transport modeling was performed by
 23 comparing the ensembles of BTCs obtained at the fine and coarse scales at the exit
 24 plane. Also, the cumulative frequency distributions obtained at the fine and coarse scales
 25 for the mean, early, median and late arrival times were compared.

1 4.5. Upscaling of retardation factor

2 The upscale of retardation factor was performed by solving the reactive solute transport
3 at the fine scale considering K , α and R as heterogeneous and uncorrelated. Solute mass
4 was released from one side of the block and collected at the opposite side and then the
5 BTCs at the exit plane were computed. From these BTCs, R was inversely determined
6 by using Eq. (13). The resulting values were considered as the equivalent ones (R_{eq}),
7 and, from them, the exponent p that yields a p -norm of the fine values that gives results
8 as close to R_{eq} as possible is chosen. Since the purpose is to observe only the effects of
9 chemical heterogeneity, R was subdivided into physically driven (related to hydraulic
10 conductivity heterogeneity) and chemically driven.

11 When solute arrived earlier in the coarse scale transport model than in the fine scale
12 solution, a calibration parameter named “fictitious” retardation factor (R_f) was added to
13 each solute transport model to retard the arrival times and improve the prediction capacity
14 of the macrodispersion method as suggested by Cassiraga et al. (2005). This retardation
15 factor does not represent chemical heterogeneity, but rather a delay associate with the
16 physical heterogeneity that is removed after upscaling. To calculate R_f , we measured the
17 solute velocity at the early, mean, median and late arrival times relative to the velocity of
18 the same problem solved with a homogeneous $R = 1$, and then we quantified R_f as the
19 ratio between the “apparently” retarded solute and the non-retarded solute for each arrival
20 time.

21 We determined an exponent p for each realization individually. The optimization of the
22 value of p was obtained using the MATLAB function called “fminbnd” based on a golden-
23 section search and parabolic interpolation (Brent, 1973; Forsythe et al., 1976) that
24 minimizes the objective function

$$\text{error}(p) = |R_{eq} - R_b|. \quad (19)$$

25 Solute transport models were then solved at the coarse-scale using the R_b determined by
26 the best p -norm. The assessment of the R upscaling was made by comparing the BTC
27 obtained at the coarse scale to the ones obtained at the fine scale. These comparisons

1 were made for the entire BTC, and for the mean, early, median and late arrival times. It
2 was quantified by the relative bias of retardation factor (RB_R), given by

$$RB_R = \frac{1}{NR} \sum_{i=1}^{NR} \left| \frac{c_{fr,i} - c_{cr,i}}{c_{fr,i}} \right| 100, \quad (20)$$

3 where $c_{fr,i}$ is the reactive solute concentration through a control plane obtained from the
4 numerical modeling at the fine scale for realization i , and $c_{cr,i}$ is the reactive solute
5 concentration through the same control plane at the coarse scale for the same realization.
6 The uncertainty analysis of the reactive solute transport modeling was performed in the
7 same way as that of the nonreactive solute transport.

8 **5. Results and discussion**

9 **5.1. Hydrodynamic dispersion upscaling**

10 The relative bias of the specific discharge during hydraulic conductivity upscaling was
11 only 0.8% indicating that the upscaling method worked well at the coarse scale in
12 reproducing the water flow obtained at the fine scale. Fig. 4 shows the BTCs of realization
13 number 30 at the fine scale and after upscaling for three situations: 1) upscaling only K ,
14 2) upscaling using macrodispersion approach, and 3) upscaling using macrodispersion
15 approach with a calibration term named fictitious retardation factor that will be discussed
16 further on.

17 As demonstrated by others in the literature (Cassiraga et al., 2005; Journel et al., 1986;
18 Scheibe and Yabusaki, 1998), upscaling only K , even using an advanced non-local
19 method, is not enough to reproduce the BTCs at the coarse scale. When only the K
20 upscaling is done, the coarse scale BTC overestimates the early arrival times and
21 underestimate the late arrival ones. Since the K upscaling worked very well, the
22 overestimation of the equivalent K could not explain such behavior. This finding was also
23 reported by Li et al. (2011b) and Fernández-García and Gómez-Hernández (2007).
24 Homogenization produces a reduction of dispersion due to a loss of K heterogeneity,
25 therefore justifying the inclusion of a term that will represent this loss: the macrodispersion
26 coefficient.

1 The macrodispersion approach was used to upscale transport at the fine scale, in order
2 to take into account the loss of dispersion caused by hydraulic conductivity upscaling.
3 Block equivalent dispersivities from scenario 2 (see Fig. 3) were used in the transport
4 equation at the coarse scale and BTCs at the control plane were determined. In Fig. 4, it
5 is noticeable that the inclusion of the macrodispersion coefficient in the transport equation
6 at the coarse scale was not enough to properly describe the heterogeneous processes
7 taking place within a block to reproduce the BTC obtained at the fine scale, as also
8 mentioned by others (Fernández-García et al., 2009; Fernández-García and Gómez-
9 Hernández, 2007; Fripiat and Holeyman, 2008). The slope of the BTC is almost the
10 same, indicating that the dispersion was quantified correctly, however, it seems that the
11 solute arrives earlier in the coarse scale transport model, underestimating the arrival
12 times. A similar result was also mentioned by Fernández-García et al. (2009) and can be
13 related to anomalous (non-Fickian) solute transport. To correct the underestimation of the
14 arrival times, the calibration parameter R_f was added. In Fig. 4, it is noticeable that the
15 reproduction at the coarse scale of the fine scale BTC is more precise and presents
16 smaller errors after the inclusion of R_f .

17 From Fig. 4, we can notice that the efficiency of the macrodispersion method is not the
18 same for the entire BTC, and, according to the solute modeling objective, the ADE
19 approach can be more or less suitable. For this reason, we investigated the results for
20 the early, mean, median and late arrival times to quantify the differences between arrival
21 times at the fine and coarse scales after macrodispersion upscaling. Fig. 5 (a - d) shows,
22 for each of the thirty realizations, the comparison of the mean time and the times when
23 5%, 50% and 95% of the concentration has arrived at the control plane computed at the
24 fine scale, and at the coarse scale after upscaling using the Macrodispersion approach.
25 It is remarkable that none of the arrival times was well reproduced at the coarse scale by
26 the macrodispersion upscaling, with the worst reproduction obtained for the early times
27 and the best one for the mean arrival times. In all situations analyzed, the
28 Macrodispersion method overestimates the concentrations at any given time. Different
29 results were obtained by Fernández-García et al. (2009), Fernández-García and Gómez-
30 Hernández (2007) and Cassiraga et al., (2005), where the macrodispersive model was
31 capable of reproducing $T_{05\%}$. In the works by these researchers, the late arrival time ($T_{95\%}$)

1 of the BTC at the coarse scale was the most poorly reproducing the fine scale values,
2 contrary to our results.

3 The performance of upscaling after the inclusion of a fictitious retardation factor was also
4 investigated for the early, mean, median and late arrival times. The results are shown in
5 Fig. 6 (a-d). Although the inclusion of a R_f improved the results, it was not enough to
6 reproduce the transport at the coarse scale for the early arrival times. Again, the best
7 results were obtained for the mean arrival times, indicating that this approach can be best
8 suited for performing, for instance, health risk analysis of contamination by drinking water.
9 Results obtained for the median and late arrival times were also good with small relative
10 bias (4.38 % and 3.92 %, respectively).

11 These results show that without the inclusion of R_f there is no R that can represent the
12 apparently anomalous transport at the coarse scale. As an alternative, upscaling may be
13 done including memory functions to describe the processes leading to slow advection
14 within a block (Fernández-García et al., 2009; Li et al., 2011b). However, after the
15 correction using a R_f , a good reproduction of the transport at the coarse scale was
16 obtained for the median, mean and late arrival times. This simple method could promptly
17 be used in daily practice, improving the quality of the solute transport predictions.

18 **5.2. Retardation factor upscaling**

19 Fig. 7 illustrates that different retardation factors must be used to reproduce different parts
20 of the BTC. Since a single R_{eq} is not able to reproduce the entire BTC, retardation factor
21 upscaling was performed considering different R_{eq} for the early, median, mean and late
22 arrival times. The equivalent retardation factor represents not only the chemical
23 heterogeneity, but also the heterogeneity related to hydraulic conductivity, evidenced by
24 the need to include a fictitious retardation factor to properly upscale hydrodynamic
25 dispersion after hydraulic conductivity upscaling. However, as here the aiming was to
26 observe only the effects of chemical heterogeneity, the effect of K heterogeneity on R ,
27 represented by R_f , was removed before the calculation of R_b ($R_b = R_{eq} / R_f$).

28 We investigated the determination of an exponent p for the ensemble of 30 realizations
29 considered altogether. The arithmetic mean ($p=1$) resulted in the smallest RB_R and,

1 therefore, was found to be the best approximate for the median, mean and late arrival
2 times. Differently, for the early arrival time the geometric mean ($p=0$) was the best
3 average. There is no clear indication of systematic under or overestimation of the results,
4 however, using a single p -exponent to predict all the curves gives errors as large as 21%.
5 Because of that, to improve the prediction quality, the block retardation factor was
6 determined using the best p exponent for each realization. Fig. 8 shows the cumulative
7 frequency distribution function of the p exponents from the different realizations found for
8 the early, median, mean and late arrival times. We can observe that they present high
9 variability, ranging from -10.25 to 12.60 with a very similar shape of their CDFs. Fig. 9
10 presents the comparison of the early, median, mean and late arrival times obtained
11 computed at the fine scale vs. the results obtained after upscaling using a different (the
12 best) p -exponent for each realization. All arrival times have a small relative bias and the
13 best result was obtained for the mean arrival time. Our result showed that the upscaling
14 of the retardation factor using a best p -exponent for each realization resulted in a very
15 good coarse-scale reproduction of the reactive transport at the fine scale.

16 **5.3. Uncertainty propagation**

17 Since exhaustive knowledge of the area of interest is unattainable due to the large spatial
18 variability of the parameters and limited sampling, we need to use a stochastic approach
19 for the quantification of uncertainty, where multiple possible scenarios (realizations) are
20 considered. When performing solute transport upscaling, the uncertainty in the upscaled
21 model must be investigated. In this sense, we evaluated how uncertainty propagates after
22 solute transport upscaling.

23 The cumulative frequency distribution function (CDF) is used to measure the uncertainty
24 about each of the different arrival times. Fig. 10 (a to d) shows the results of the
25 uncertainty reproduction after macrodispersion upscaling by comparing the CDFs of the
26 early (a), median (b), mean (c) and late (d) arrival times at both scales, with and without
27 inclusion of the fictitious retardation factor. We can see that the CDF without R_f is
28 displaced to the left, indicating an overestimation of the concentrations. The inclusion of
29 R_f resulted in a much better reproduction of all arrival times. The uncertainty, related to
30 the slope of the CDF, was well reproduced for all arrival times for the models with and

1 without the inclusion of the fictitious retardation factor. However, for the early arrival time,
2 even with the inclusion of the fictitious retardation factor there was an overestimation of
3 the concentrations. These results show that the inclusion of R_f in hydrodynamic dispersion
4 upscaling was necessary for the correct reproduction of all arrival times but had no
5 influence on the uncertainty propagation.

6 We also evaluated the uncertainty propagation after R upscaling. The results are shown
7 in Fig. 11, where the CDF of the early, median, mean and late arrival times obtained at
8 the fine scale are compared with those obtained at the coarse scale using the best
9 exponent p for each realization. We can notice that the larger the arrival time, the larger
10 the uncertainty. The uncertainty was properly propagated for all arrival times. However,
11 the upscaling of R at the late arrival time showed an overestimation of the concentrations.

12 **6. Conclusions**

13 Stochastic solute transport upscaling using real data from a tropical soil was performed.
14 Upscaling of hydraulic conductivity, hydrodynamic dispersion, and retardation factor were
15 done using different techniques of varying complexity. Macrodispersion coefficients were
16 determined considering heterogeneous hydraulic conductivities and dispersivities at the
17 local scale. Upscaling of retardation factor was made by using the p -norm approach.
18 Uncertainty analyses were also performed to evaluate how uncertainty propagates after
19 upscaling.

20 Upscaling of hydraulic conductivity only, even when using a non-local method, was not
21 enough to reproduce the BTCs at the coarse scale; there is a need to include a
22 macrodispersion coefficient. The Macrodispersion method can be used directly to quantify
23 both the effects of heterogeneity of dispersivity and hydraulic conductivity at the local
24 scale with a small relative bias. However, the inclusion of the macrodispersion coefficient
25 in the transport equation at the coarse scale was not enough to properly describe the
26 heterogeneous processes at the coarse scale. There is a need to include a calibration
27 parameter, a fictitious retardation factor, for the macrodispersion model to get a small
28 relative bias. The retardation factor was well reproduced at the coarse scale when a
29 specific p exponent was used for each realization. The best results were obtained for the

1 mean arrival times, while the early arrival time resulted in the worst relative bias. The
2 uncertainty was properly propagated after hydrodynamic dispersion upscaling, however,
3 only when a fictitious retardation factor was included there was no overestimation of the
4 contamination. Retardation factor upscaling propagated well the uncertainty for all arrival
5 times. Lastly, the results show that solute transport upscaling can be incorporated into
6 practice by the numerical modeler even using commercial codes, but it may need some
7 corrections with the need to include a fictitious retardation factor in some cases.

8

1 **Acknowledgments**

2

3 The authors thank the financial support by the Brazilian National Council for Scientific and
4 Technological Development (CNPq) (Project 401441/2014-8). The doctoral fellowship
5 award to the first author by the Coordination of Improvement of Higher Level Personnel
6 (CAPES) is acknowledged. The first author also thanks the international mobility grant
7 awarded by CNPq, through the Sciences Without Borders program (grant number:
8 200597/2015-9). The international mobility grant awarded by Santander Mobility in
9 cooperation with the University of Sao Paulo is also acknowledged. DHI-WASI is
10 gratefully thanked for providing a FEFLOW license.

1 **References**

- 2 Ahuja, L.R., Naney, J.W., Green, R.E., Nielsen, D.R., 1984. Macroporosity to
3 Characterize Spatial Variability of Hydraulic Conductivity and Effects of Land
4 Management1. *Soil Sci. Soc. Am. J.* 48:, 699.
5 <https://doi.org/10.2136/sssaj1984.03615995004800040001x>
- 6 Azevedo, A.A.B. de, Pressinotti, M.M.N., Massoli, M., 1981. Sedimentological studies of
7 the Botucatu and Pirambóia formations in the region of Santa Rita do Passa Quatro
8 (In portuguese). *Rev. do Inst. Geológico* 2:, 31–38. <https://doi.org/10.5935/0100-929X.19810003>
- 10 Bellin, A., Lawrence, A.E., Rubin, Y., 2004. Models of sub-grid variability in numerical
11 simulations of solute transport in heterogeneous porous formations: three-
12 dimensional flow and effect of pore-scale dispersion. *Stoch. Environ. Res. Risk*
13 *Assess.* 18:, 31–38. <https://doi.org/10.1007/s00477-003-0164-2>
- 14 Brent, R.P., 1973. *Algorithms for Minimization without Derivatives*. Prentice Hall,
15 Englewood cliffs, New Jersey.
- 16 Brusseau, M.L., 1998. Non-ideal transport of reactive solutes in heterogeneous porous
17 media: 3. model testing and data analysis using calibration versus prediction. *J.*
18 *Hydrol.* 209:, 147–165. [https://doi.org/10.1016/S0022-1694\(98\)00121-8](https://doi.org/10.1016/S0022-1694(98)00121-8)
- 19 Brusseau, M.L., Srivastava, R., 1999. Nonideal transport of reactive solutes in
20 heterogeneous porous media: 4. Analysis of the Cape Cod Natural-Gradient Field
21 Experiment. *Water Resour. Res.* 35:, 1113–1125.
22 <https://doi.org/10.1029/1998WR900019>
- 23 Brutsaert, W., 1967. Some methods of calculating unsaturated permeability. *Trans.*
24 *ASAE* 10:, 400–404.
- 25 Cadini, F., De Sanctis, J., Bertoli, I., Zio, E., 2013. Upscaling of a dual-permeability
26 Monte Carlo simulation model for contaminant transport in fractured networks by
27 genetic algorithm parameter identification. *Stoch. Environ. Res. Risk Assess.* 27:,
28 505–516. <https://doi.org/10.1007/s00477-012-0595-8>

- 1 Cambardella, C.A., Moorman, T.B., Parkin, T.B., Karlen, D.L., Novak, J.M., Turco, R.F.,
2 Konopka, A.E., 1994. Field-Scale Variability of Soil Properties in Central Iowa Soils.
3 Soil Sci. Soc. Am. J. 58:, 1501.
4 <https://doi.org/10.2136/sssaj1994.03615995005800050033x>
- 5 Capilla, J.E., Rodrigo, J., Gómez-Hernández, J.J., 1999. Simulation of non-Gaussian
6 transmissivity fields honoring piezometric data and integrating soft and secondary
7 information. Math. Geol. 31:, 907–927. <https://doi.org/10.1023/A:1007580902175>
- 8 Cassiraga, E.F., Fernández-García, D., Gómez-Hernández, J.J., 2005. Performance
9 assessment of solute transport upscaling methods in the context of nuclear waste
10 disposal. Int. J. Rock Mech. Min. Sci. 42:, 756–764.
11 <https://doi.org/10.1016/j.ijrmms.2005.03.013>
- 12 Corey, A.T., 1977. Mechanics of heterogeneous fluids in porous media. Mech. Heterog.
13 fluids porous media.
- 14 Dagan, G., 2004. On application of stochastic modeling of groundwater flow and
15 transport. Stoch. Environ. Res. Risk Assess. 18:. [https://doi.org/10.1007/s00477-](https://doi.org/10.1007/s00477-004-0191-7)
16 [004-0191-7](https://doi.org/10.1007/s00477-004-0191-7)
- 17 Dagan, G., 1989. Flow and Transport in Porous Formations. Springer Berlin Heidelberg,
18 Berlin, Heidelberg. <https://doi.org/10.1007/978-3-642-75015-1>
- 19 Deng, H., Dai, Z., Wolfsberg, A. V., Ye, M., Stauffer, P.H., Lu, Z., Kwicklis, E., 2013.
20 Upscaling retardation factor in hierarchical porous media with multimodal reactive
21 mineral facies. Chemosphere 91:, 248–257.
22 <https://doi.org/10.1016/j.chemosphere.2012.10.105>
- 23 Diersch, H.-J.G., 2014. Finite Element Modeling of Flow, Mass and Heat Transport in
24 Porous and Fractured Media. <https://doi.org/10.1007/978-3-642-38739-5>
- 25 Dippenaar, M.A., 2014. Porosity Reviewed: Quantitative Multi-Disciplinary
26 Understanding, Recent Advances and Applications in Vadose Zone Hydrology.
27 Geotech. Geol. Eng. 32:, 1–19. <https://doi.org/10.1007/s10706-013-9704-9>
- 28 Fagundes, J.R.T., Zuquette, L.V., 2011. Sorption behavior of the sandy residual

- 1 unconsolidated materials from the sandstones of the Botucatu Formation, the main
2 aquifer of Brazil. *Environ. Earth Sci.* 62:, 831–845. [https://doi.org/10.1007/s12665-](https://doi.org/10.1007/s12665-010-0570-y)
3 010-0570-y
- 4 Fernàndez-Garcia, D., Gómez-Hernández, J.J., 2007. Impact of upscaling on solute
5 transport: Traveltimes, scale dependence of dispersivity, and propagation of
6 uncertainty. *Water Resour. Res.* 43:. <https://doi.org/10.1029/2005WR004727>
- 7 Fernàndez-Garcia, D., Llerar-Meza, G., Gómez-Hernández, J.J., 2009. Upscaling
8 transport with mass transfer models: Mean behavior and propagation of
9 uncertainty. *Water Resour. Res.* 45:. <https://doi.org/10.1029/2009WR007764>
- 10 Feyen, L., Gómez-Hernández, J.J., Ribeiro, P.J., Beven, K.J., De Smedt, F., 2003a. A
11 Bayesian approach to stochastic capture zone delineation incorporating tracer
12 arrival times, conductivity measurements, and hydraulic head observations. *Water*
13 *Resour. Res.* 39:. <https://doi.org/10.1029/2002WR001544>
- 14 Feyen, L., Ribeiro, P.J., Gómez-Hernández, J.J., Beven, K.J., De Smedt, F., 2003b.
15 Bayesian methodology for stochastic capture zone delineation incorporating
16 transmissivity measurements and hydraulic head observations. *J. Hydrol.* 271:,
17 156–170. [https://doi.org/10.1016/S0022-1694\(02\)00314-1](https://doi.org/10.1016/S0022-1694(02)00314-1)
- 18 Forsythe, G.E., Malcolm, M.A., Moler, C.B., 1976. *Computer Methods for Mathematical*
19 *Computations*. Englewood Cliffs. Prentice-Hall, Englewood cliffs, New Jersey.
20 <https://doi.org/0131653326>
- 21 Freeze, R., Cherry, J., 1979. *Groundwater* (p. 604). PrenticeHall Inc Englewood cliffs,
22 New Jersey.
- 23 Frippiat, C.C., Holeyman, A.E., 2008. A comparative review of upscaling methods for
24 solute transport in heterogeneous porous media. *J. Hydrol.* 362:, 150–176.
25 <https://doi.org/10.1016/j.jhydrol.2008.08.015>
- 26 Fu, J., Gómez-Hernández, J.J., 2009. Uncertainty assessment and data worth in
27 groundwater flow and mass transport modeling using a blocking Markov chain
28 Monte Carlo method. *J. Hydrol.* 364:, 328–341.

- 1 <https://doi.org/10.1016/j.jhydrol.2008.11.014>
- 2 Gelhar, L.W., Axness, C.L., 1983. Three-dimensional stochastic analysis of
3 macrodispersion in aquifers. *Water Resour. Res.* 19:, 161–180.
4 <https://doi.org/10.1029/WR019i001p00161>
- 5 Gelhar, L.W., Welty, C., Rehfeldt, K.R., 1992. A critical review of data on field-scale
6 dispersion in aquifers. *Water Resour. Res.* 28:, 1955–1974.
7 <https://doi.org/10.1029/92WR00607>
- 8 Giacheti, H.L., Rohm, S.A., Nogueira, J.B., Cintra, J.C.A., 1993. Geotechnical
9 properties of the Cenozoic sediment (In portuguese), in: Albiero, J.H., Cintra, J.C.A.
10 (Eds.), *Soil from the Interior of São Paulo*. ABMS, Sao Paulo, pp. 143–175.
- 11 Gómez-Hernandez, J.J., 1990. A stochastic approach to the simulation of block
12 conductivity fields conditional upon data measured at a smaller scale. Stanford
13 University.
- 14 Gómez-Hernández, J.J., Fu, J., Fernandez-Garcia, D., 2006. Upscaling retardation
15 factors in 2-D porous media, in: Bierkens, M.F.P., Gehrels, J.C., Kovar, K. (Eds.),
16 *Calibration and Reliability in Groundwater Modelling : From Uncertainty to Decision*
17 *Making : Proceedings of the ModelCARE 2005 Conference Held in The Hague, the*
18 *Netherlands, 6-9 June, 2005*. IAHS Publication, pp. 130–136.
- 19 Gómez-Hernández, J.J., Gorelick, S.M., 1989. Effective groundwater model parameter
20 values: Influence of spatial variability of hydraulic conductivity, leakage, and
21 recharge. *Water Resour. Res.* 25:, 405–419.
- 22 Gómez-Hernández, J.J., Journel, A., 1993. Joint Sequential Simulation of
23 MultiGaussian Fields, in: *Geostatistics Tróia '92*. pp. 85–94.
24 https://doi.org/10.1007/978-94-011-1739-5_8
- 25 Gómez-Hernández, J.J., Wen, X.-H., 1994. Probabilistic assessment of travel times in
26 groundwater modeling. *Stoch. Hydrol. Hydraul.* 8:, 19–55.
27 <https://doi.org/10.1007/BF01581389>
- 28 Goovaerts, P., 1999. *Geostatistics in soil science: State-of-the-art and perspectives*.

1 Geoderma 89:, 1–45. [https://doi.org/10.1016/S0016-7061\(98\)00078-0](https://doi.org/10.1016/S0016-7061(98)00078-0)

2 Griffiths, D. V., Fenton, G. a., 2008. Risk Assessment in Geotechnical Engineering.

3 Jarvis, N.J., 2007. A review of non-equilibrium water flow and solute transport in soil
4 macropores: Principles, controlling factors and consequences for water quality. Eur.
5 J. Soil Sci. 58:, 523–546. <https://doi.org/10.4141/cjss2011-050>

6 Jellali, S., Diamantopoulos, E., Kallali, H., Bennaceur, S., Anane, M., Jedidi, N., 2010.
7 Dynamic sorption of ammonium by sandy soil in fixed bed columns: Evaluation of
8 equilibrium and non-equilibrium transport processes. J. Environ. Manage. 91:, 897–
9 905. <https://doi.org/10.1016/j.jenvman.2009.11.006>

10 Journal, A., Deutsch, C., Desbarats, A., 1986. Power averaging for block effective
11 permeability. Proc. SPE Calif. Reg. Meet. <https://doi.org/10.2118/15128-MS>

12 Journal, A.G., Gomez-Hernandez, J.J., 1993. Stochastic Imaging of the Wilmington
13 Clastic Sequence. SPE Form. Eval. 8:, 33–40. <https://doi.org/10.2118/19857-PA>

14 Kronberg, B.I., Fyfe, W.S., Leonardos, O.H., Santos, A.M., 1979. The chemistry of
15 some Brazilian soils: Element mobility during intense weathering. Chem. Geol. 24:,
16 211–229. [https://doi.org/10.1016/0009-2541\(79\)90124-4](https://doi.org/10.1016/0009-2541(79)90124-4)

17 Lake, L.W., 1988. The Origins of Anisotropy (includes associated papers 18394 and
18 18458). J. Pet. Technol. 40:, 395–396. <https://doi.org/10.2118/17652-PA>

19 Lawrence, A.E., Rubin, Y., 2007. Block-effective macrodispersion for numerical
20 simulations of sorbing solute transport in heterogeneous porous formations. Adv.
21 Water Resour. 30:, 1272–1285. <https://doi.org/10.1016/j.advwatres.2006.11.005>

22 Lemke, L.D., Barrack II, W.A., Abriola, L.M., Goovaerts, P., 2004. Matching Solute
23 Breakthrough with Deterministic and Stochastic Aquifer Models. Groundwater 42:,
24 920–934.

25 Li, L., Zhou, H., Gómez-Hernández, J.J., 2011a. A comparative study of three-
26 dimensional hydraulic conductivity upscaling at the macro-dispersion experiment
27 (MADE) site, Columbus Air Force Base, Mississippi (USA). J. Hydrol. 404:, 278–

1 293. <https://doi.org/10.1016/j.jhydrol.2011.05.001>

2 Li, L., Zhou, H., Gómez-Hernández, J.J., 2011b. Transport upscaling using multi-rate
3 mass transfer in three-dimensional highly heterogeneous porous media. *Adv.*
4 *Water Resour.* 34:, 478–489. <https://doi.org/10.1016/j.advwatres.2011.01.001>

5 Logsdon Keller, K.E., Moorman, T.B., 2002. Measured and Predicted Solute Leaching
6 from Multiple Undisturbed Soil Columns. *Soil Sci. Soc. am. J.* 66:, 686–695.
7 <https://doi.org/10.2136/sssaj2002.6860>

8 Lourens, A., van Geer, F.C., 2016. Uncertainty propagation of arbitrary probability
9 density functions applied to upscaling of transmissivities. *Stoch. Environ. Res. Risk*
10 *Assess.* 30:, 237–249. <https://doi.org/10.1007/s00477-015-1075-8>

11 Mahapatra, I.C., Singh, K.N., Pillai, K.G., Bapat, S.R., 1985. Rice soils and their
12 management. *Indian J. Agron.* 1–41.

13 Morakinyo, J.A., Mackay, R., 2006. Geostatistical modelling of ground conditions to
14 support the assessment of site contamination. *Stoch. Environ. Res. Risk Assess.*
15 20:, 106–118. <https://doi.org/10.1007/s00477-005-0015-4>

16 Moslehi, M., de Barros, F.P.J., Ebrahimi, F., Sahimi, M., 2016. Upscaling of solute
17 transport in disordered porous media by wavelet transformations. *Adv. Water*
18 *Resour.* 96:, 180–189. <https://doi.org/10.1016/j.advwatres.2016.07.013>

19 Osinubi, K. 'J., Nwaiwu, C.M., 2005. Hydraulic Conductivity of Compacted Lateritic Soil.
20 *J. Geotech. Geoenvironmental Eng.* 131:, 1034–1041.
21 [https://doi.org/10.1061/\(ASCE\)1090-0241\(2005\)131:8\(1034\)](https://doi.org/10.1061/(ASCE)1090-0241(2005)131:8(1034))

22 Remy, N., 2004. SGeMS: Stanford Geostatistical Modeling Software. *Softw. Man.*
23 https://doi.org/10.1007/978-1-4020-3610-1_89

24 Renard, P., de Marsily, G., 1997. Calculating equivalent permeability: a review. *Adv.*
25 *Water Resour.* 20:, 253–278. [https://doi.org/10.1016/S0309-1708\(96\)00050-4](https://doi.org/10.1016/S0309-1708(96)00050-4)

26 Robin, M.J.L., Sudicky, E.A., Gillham, R.W., Kachanoski, R.G., 1991. Spatial Variability
27 of Strontium Distribution Coefficients and Their Correlation With Hydraulic

- 1 Conductivity in the Canadian Forces Base Borden Aquifer. *Water Resour. Res.* 27:,
2 2619–2632. <https://doi.org/10.1029/91WR01107>
- 3 Salamon, P., Fernàndez-Garcia, D., Gómez-Hernández, J.J., 2007. Modeling tracer
4 transport at the MADE site: The importance of heterogeneity. *Water Resour. Res.*
5 43:. <https://doi.org/10.1029/2006WR005522>
- 6 Sánchez-Vila, X., Carrera, J., Girardi, J.P., 1996. Scale effects in transmissivity. *J.*
7 *Hydrol.* 183:, 1–22. [https://doi.org/10.1016/S0022-1694\(96\)80031-X](https://doi.org/10.1016/S0022-1694(96)80031-X)
- 8 Scheibe, T., Yabusaki, S., 1998. Scaling of flow and transport behavior in
9 heterogeneous groundwater systems. *Adv. Water Resour.* 22:, 223–238.
10 [https://doi.org/10.1016/S0309-1708\(98\)00014-1](https://doi.org/10.1016/S0309-1708(98)00014-1)
- 11 Selvadurai, P.A., Selvadurai, A.P.S., 2014. On the effective permeability of a
12 heterogeneous porous medium: the role of the geometric mean. *Philos. Mag.* 94:,
13 2318–2338. <https://doi.org/10.1080/14786435.2014.913111>
- 14 Shackelford, C.D., 1994. Critical concepts for column testing. *J. Geotech. Eng.* 120:,
15 1804–1828. [https://doi.org/10.1016/0148-9062\(95\)96996-O](https://doi.org/10.1016/0148-9062(95)96996-O)
- 16 Šimůnek, J., van Genuchten, M.T., Šejna, M., Toride, N., Leij, F.J., 1999. The
17 STANMOD Computer Software for Evaluating Solute Transport in Porous Media
18 Using Analytical Solutions of Convection-Dispersion Equation. Riverside, California.
- 19 Taskinen, A., Sirviö, H., Bruen, M., 2008. Modelling effects of spatial variability of
20 saturated hydraulic conductivity on autocorrelated overland flow data: linear mixed
21 model approach. *Stoch. Environ. Res. Risk Assess.* 22:, 67–82.
22 <https://doi.org/10.1007/s00477-006-0099-5>
- 23 Tuli, A., Hopmans, J.W., Rolston, D.E., Moldrup, P., 2005. Comparison of Air and Water
24 Permeability between Disturbed and Undisturbed Soils. *Soil Sci. Soc. Am. J.* 69:,
25 1361. <https://doi.org/10.2136/sssaj2004.0332>
- 26 Tyukhova, A.R., Willmann, M., 2016. Conservative transport upscaling based on
27 information of connectivity. *Water Resour. Res.* 52:, 6867–6880.
28 <https://doi.org/10.1002/2015WR018331>

- 1 van Genuchten, M.T., 1980. Determining transport parameters from solute
2 displacement experiments.
- 3 Vanderborght, J., Timmerman, A., Feyen, J., 2000. Solute Transport for Steady-State
4 and Transient Flow in Soils with and without Macropores. *Soil Sci. Soc. Am. J.* 64:,
5 1305–1317. <https://doi.org/10.2136/sssaj2000.6441305x>
- 6 Vanmarcke, E., 1983. *Random Fields: Analysis and Synthesis*.
- 7 Vishal, V., Leung, J.Y., 2017. Statistical scale-up of 3D particle-tracking simulation for
8 non-Fickian dispersive solute transport modeling. *Stoch. Environ. Res. Risk*
9 *Assess.* <https://doi.org/10.1007/s00477-017-1501-1>
- 10 Wen, X.-H., Gómez-Hernández, J.J., 1996. Upscaling hydraulic conductivities in
11 heterogeneous media: An overview. *J. Hydrol.* 183:, ix–xxxii.
12 [https://doi.org/10.1016/S0022-1694\(96\)80030-8](https://doi.org/10.1016/S0022-1694(96)80030-8)
- 13 Wen, X.H., Capilla, J.E., Deutsch, C.V., Gómez-Hernández, J.J., Cullick, A.S., 1999. A
14 program to create permeability fields that honor single-phase flow rate and
15 pressure data. *Comput. Geosci.* 25:, 217–230. [https://doi.org/10.1016/S0098-](https://doi.org/10.1016/S0098-3004(98)00126-5)
16 [3004\(98\)00126-5](https://doi.org/10.1016/S0098-3004(98)00126-5)
- 17 Wen, X.H., Gómez-Hernández, J.J., 1998. Numerical modeling of macrodispersion in
18 heterogeneous media: a comparison of multi-Gaussian and non-multi-Gaussian
19 models. *J. Contam. Hydrol.* 30:, 129–156. [https://doi.org/10.1016/S0169-](https://doi.org/10.1016/S0169-7722(97)00035-1)
20 [7722\(97\)00035-1](https://doi.org/10.1016/S0169-7722(97)00035-1)
- 21 Wilding, L.P., Drees, L.R., 1983. Spatial variability and pedology, in: Wilding, L.P.,
22 Smeck, N.E., Hall, G.F. (Eds.), *Pedogenesis and Soil Taxonomy : The Soil Orders*.
23 Elsevier, Netherlands, pp. 83–116.
- 24 Willmann, M., Carrera, J., Guadagnini, A., 2006. Block-upscaling of transport in
25 heterogeneous aquifers. h2ogeo.upc.edu 1–7.
- 26 Xu, Z., Meakin, P., 2013. Upscaling of solute transport in heterogeneous media with
27 non-uniform flow and dispersion fields. *Appl. Math. Model.* 37:, 8533–8542.
28 <https://doi.org/10.1016/j.apm.2013.03.070>

1 Zech, A., Attinger, S., Cvetkovic, V., Dagan, G., Dietrich, P., Fiori, A., Rubin, Y.,
2 Teutsch, G., 2015. Is unique scaling of aquifer macrodispersivity supported by field
3 data? *Water Resour. Res.* 51:, 7662–7679. <https://doi.org/10.1002/2015WR017220>

4 Zhou, H., Li, L., Gómez-Hernández, J.J., 2010. Three-dimensional hydraulic
5 conductivity upscaling in groundwater modeling. *Comput. Geosci.* 36:, 1224–1235.
6 <https://doi.org/10.1016/j.cageo.2010.03.008>

7 Zhou, H., Li, L., Hendricks Franssen, H.-J., Gómez-Hernández, J.J., 2012. Pattern
8 Recognition in a Bimodal Aquifer Using the Normal-Score Ensemble Kalman Filter.
9 *Math. Geosci.* 44:, 169–185. <https://doi.org/10.1007/s11004-011-9372-3>

10

11

1 **List of Figures**

2 Fig. 1 Realization number 1 of $\ln K$ (a), n (b), $\ln \alpha$ (c) and R (d) at fine scale **(color should**
3 **be used)**

4 Fig. 2 Sketch of solute transport models indicating the source zone (purple rectangle) and
5 the exit control plane where mass concentration was measured **(color should be used)**

6 Fig. 3 Cross-plot between block equivalent dispersivity (α_b) determined using scenario 1
7 and scenario 2

8 Fig. 4 Breakthrough curves in realization number 30 at the fine scale and after upscaling
9 for three situations: 1) upscaling only K , 2) upscaling using the macrodispersion
10 approach, and 3) upscaling using the macrodispersion approach with a fictitious
11 retardation factor

12 Fig. 5 Comparison of early (a), median (b), mean (c) and late (d) arrival times obtained
13 from the model performed at the fine-scale versus the results obtained at the coarse scale
14 after upscaling using macrodispersion coefficients

15 Fig. 6 Comparison of the early (a), median (b), mean (c) and late (d) arrival times obtained
16 from the model performed at the fine scale versus the results obtained after upscaling
17 using macrodispersion coefficients and a fictitious retardation factor

18 Fig. 7 Breakthrough curves for realization number 30 at the fine scale and breakthrough
19 curves computed at the coarse scale using three different block retardation factors, aimed
20 at the reproduction of the early, median and late arrival times **(color should be used)**

21 Fig. 8 Cumulative frequency distribution function of p exponent for early, median, mean
22 and late arrival times for 30 realizations

1

2 Fig. 9 Comparison of the early (a), median (b), mean (c) and late (d) arrival times obtained
3 from the model performed at fine-scale versus the results obtained after upscaling using
4 the best p exponent for the entire ensemble

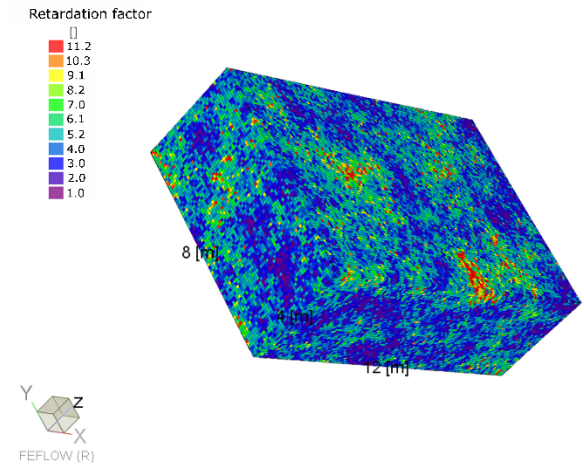
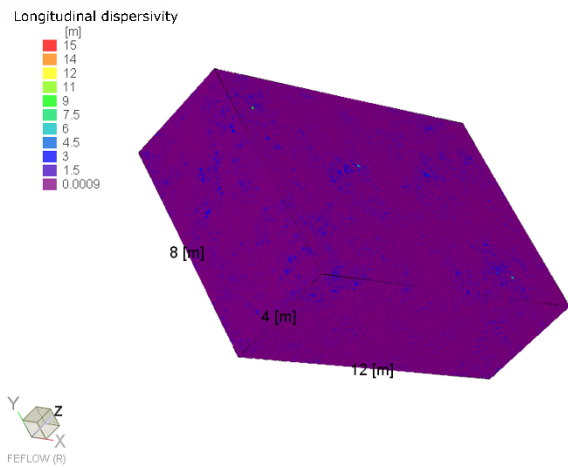
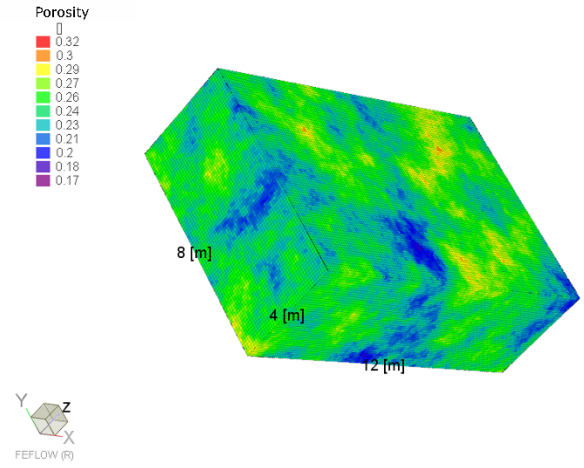
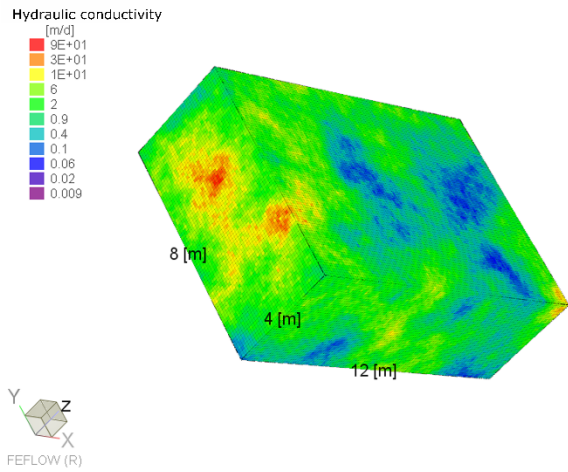
5 Fig. 10 Cumulative frequency distribution functions of the early (a), median (b), mean (c)
6 and late (d) arrival times obtained from the nonreactive BTCs computed at the fine scale
7 versus the results obtained after upscaling using only macrodispersion coefficients and
8 using macrodispersion coefficients plus a fictitious retardation factor

9 Fig. 11 Cumulative frequency distribution of the early, median, mean and late arrival times
10 obtained from the reactive BTCs before and after upscaling using the best p exponent for
11 each realization

12

1 **Fig. 1**

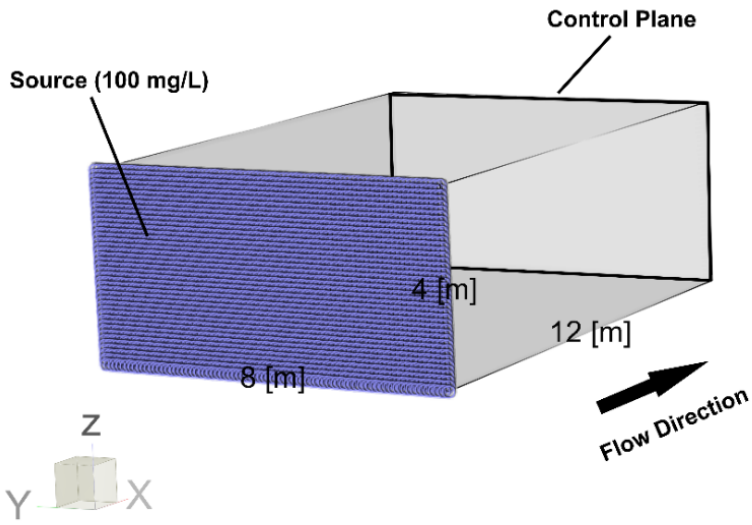
2



3

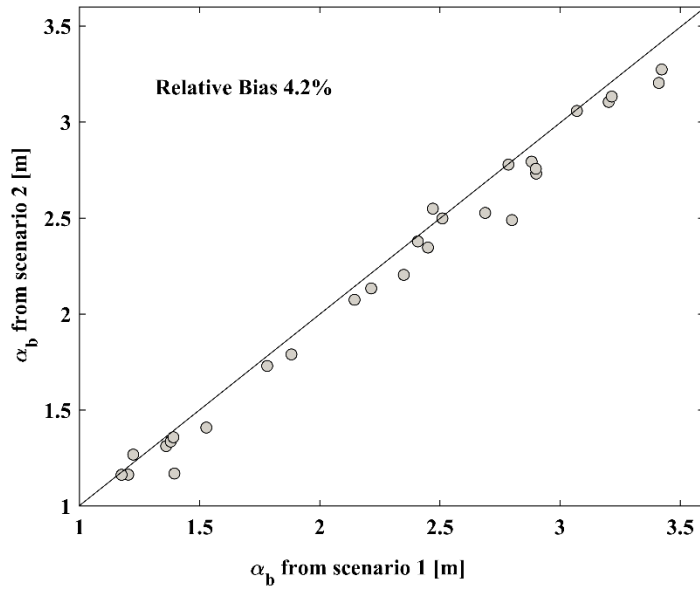
4

1 Fig. 2



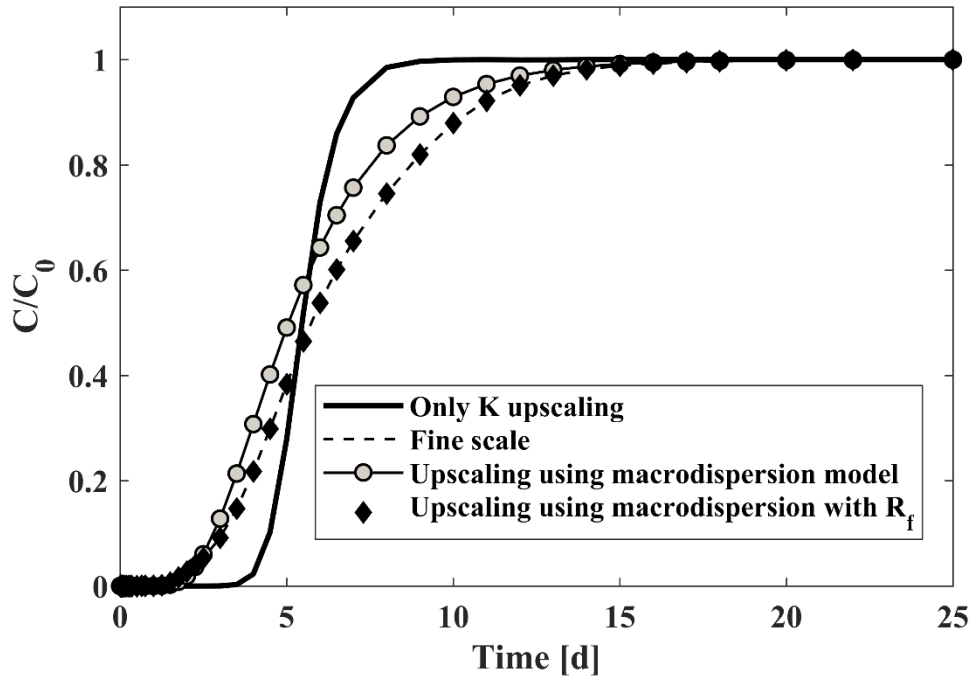
2 FEFLOW (R)

1 **Fig. 3**



2

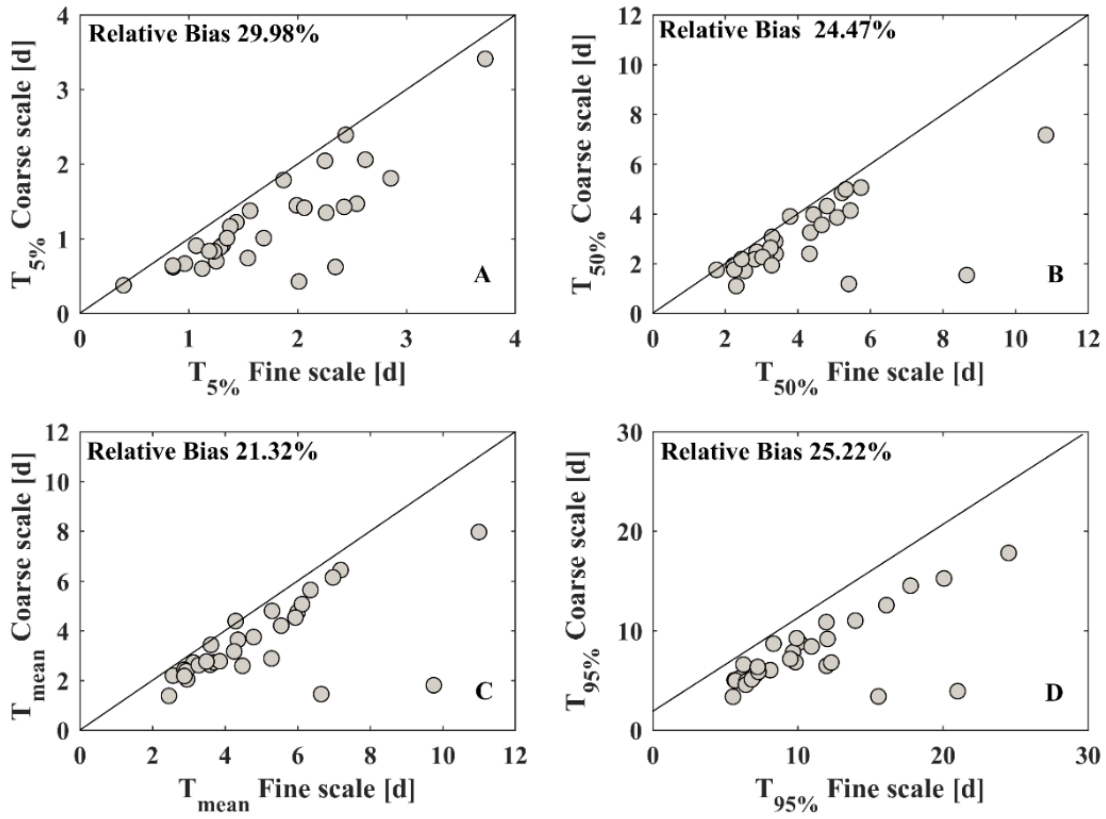
1 Fig. 4



2

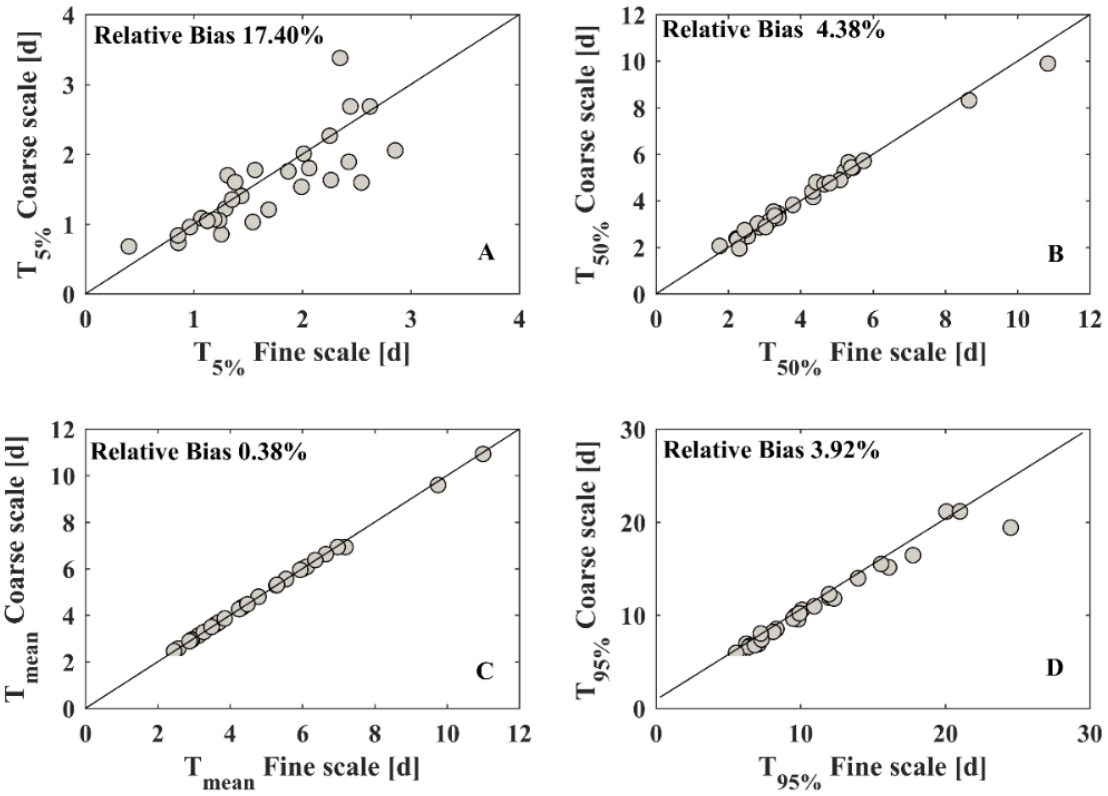
3

1 **Fig. 5**



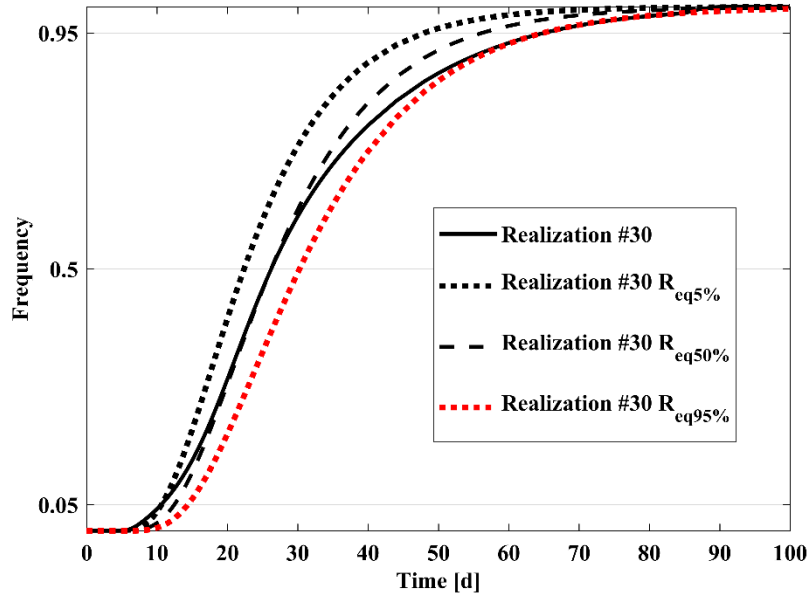
2

1 **Fig. 6**



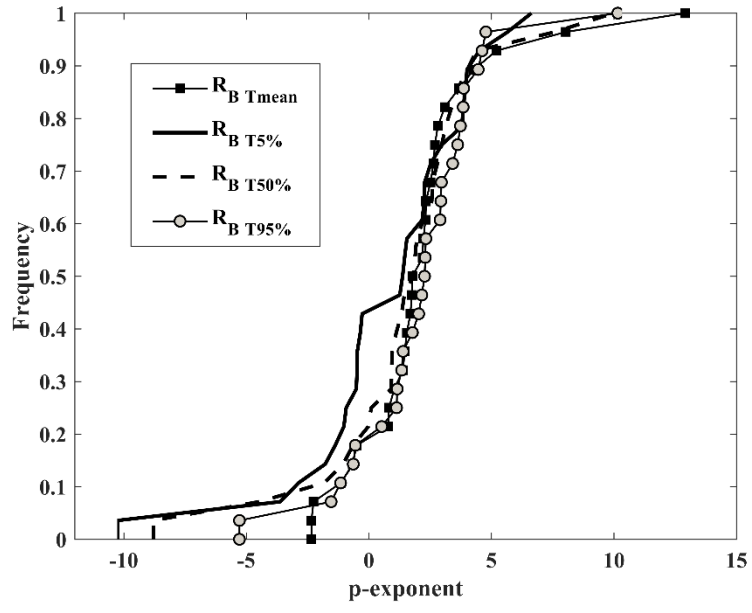
2

1 **Fig. 7**



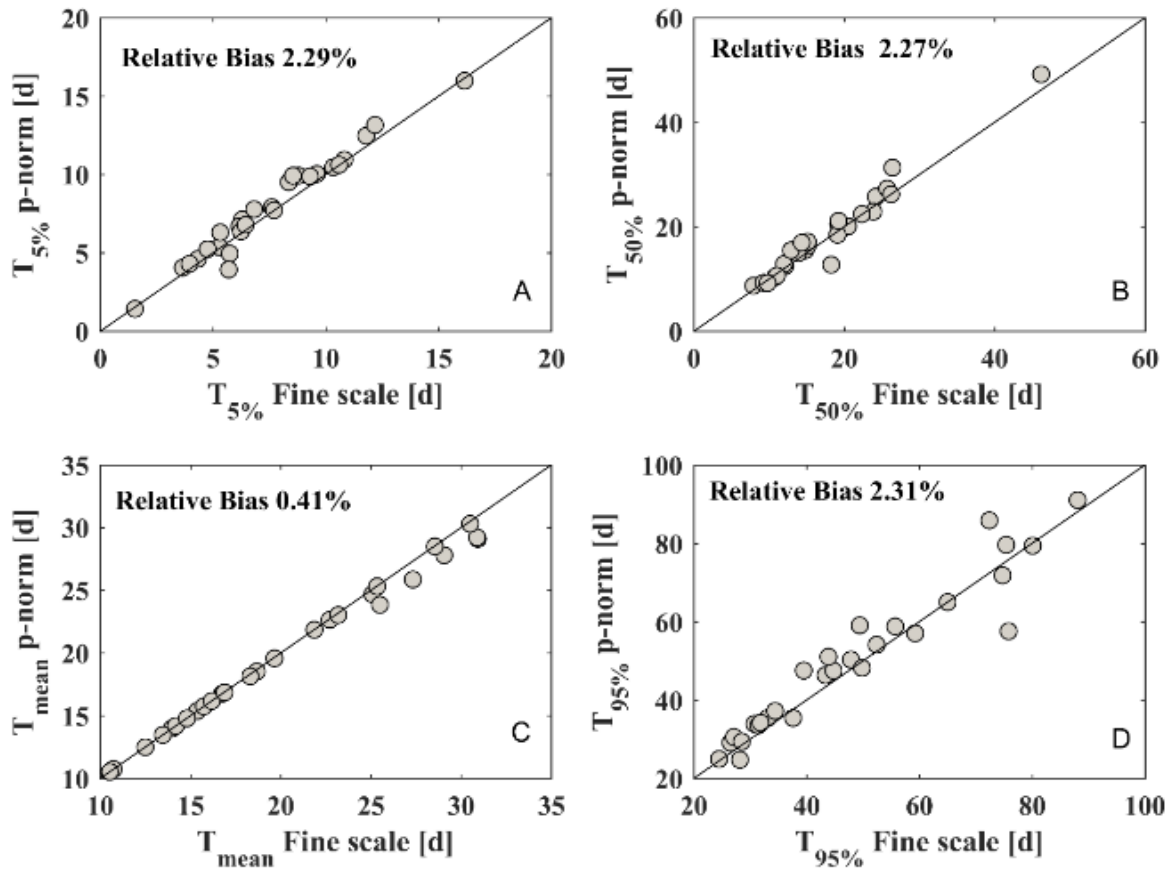
2

1 **Fig. 8**



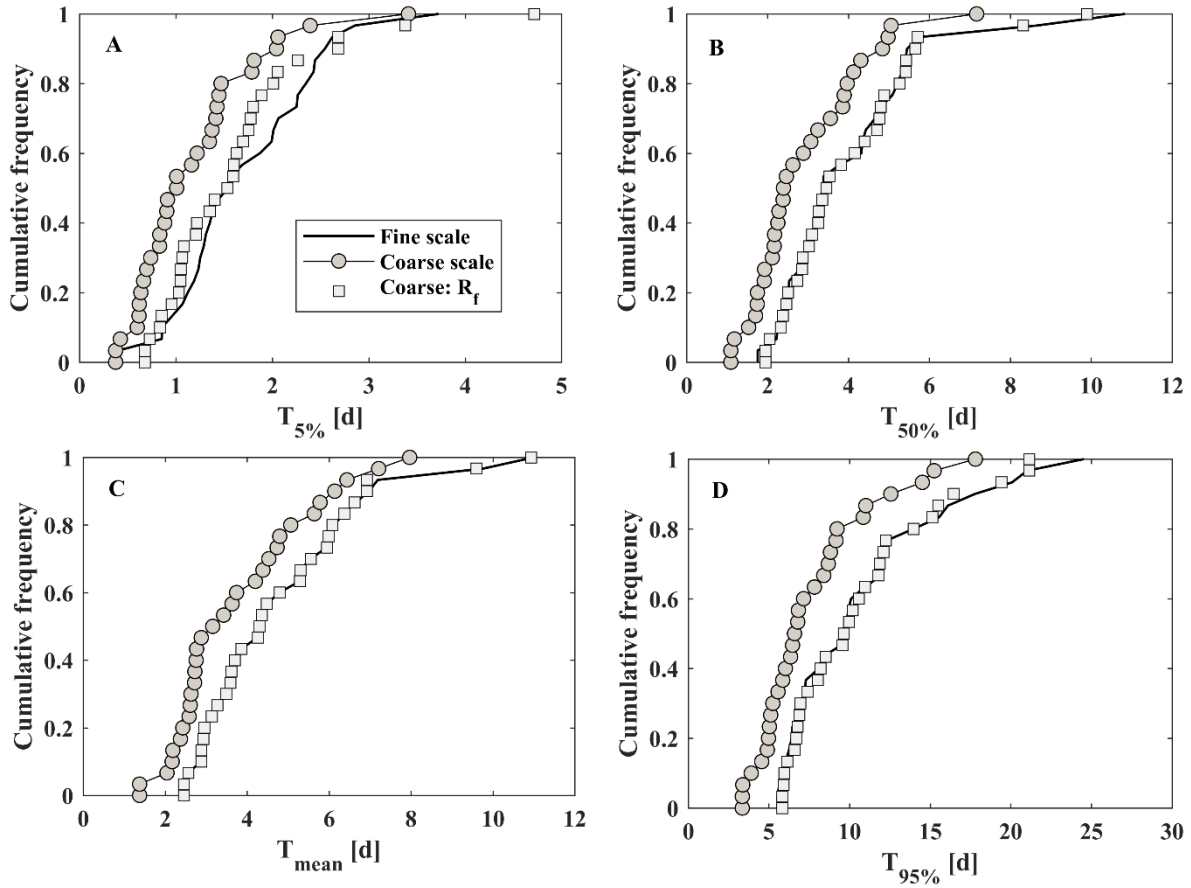
2

1 Fig. 9



2

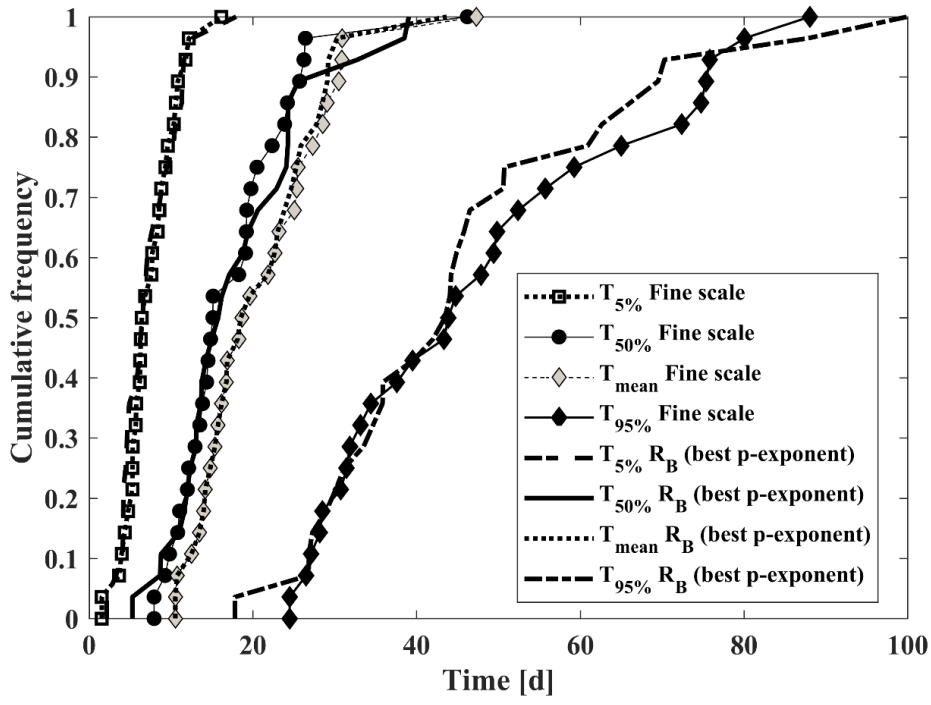
1 **Fig. 10**



2

3

1 Fig. 11



2

3

1 **List of Tables**

2 Table 1 Summary statistics of the random variables

3 Table 2 Parameters of the variogram models

4 Table 3 Scenarios used to determine the block equivalent dispersivity

1 Table 1

Variable	Mean	SD	CV
K [m d ⁻¹]	1.35	1.65	1.26
lnK [ln(m d ⁻¹)]	-0.38	1.25	n.d
n []	0.25	0.02	0.08
α [m]	0.18	0.19	1.05
lnα [ln(m)]	-2.21	1.11	n.d
R []	5.37	5.10	0.95

2 SD: standard deviation, CV: coefficient of variation, n.d: undetermined, K: hydraulic conductivity;

3 n: porosity, R: retardation factor, α: dispersivity

1 Table 2

Variable	Model	Nugget	Sill	Range (m)
lnK	Spherical	0.00	1.0	4.0
n	Spherical	0.00	1.0	3.0
ln α	Spherical	0.50	0.50	3.0
R	Spherical	0.55	0.45	3.3

2 K: hydraulic conductivity; n: porosity, R: retardation factor, α : dispersivity

3

1 Table 3

Scenario	K (at fine scale)	α (at fine scale)	Initial Result	Result
Scenario 1	Homogeneous	Heterogeneous	α_{eq}	α_b
	Heterogeneous	Homogeneous	A_i	
Scenario 2	Heterogeneous	Heterogeneous	α_b	α_b

2 α_{eq} : equivalent fine-scale local dispersivity; A_i : macrodispersivity term; α_b : block equivalent
 3 dispersivity.